

# Essay on Magnetic-Wind Mills

## Part III : Pathway for energy transfer

J.L. Duarte

Dept. Electrical Engineering (Ret.)  
Eindhoven University of Technology  
The Netherlands

**Abstract**—An attempt is made to describe that mechanical vibrations are not only responsible for evoking spacetime resonances, as Einstein-Cartan-Evans theory predicts, but could also provide a possible interface for transferring energy from the quantum vacuum to a rotating shaft.

### I. INTRODUCTION

The assembly around a magnetic-wind mill, presented in [1], may appear unusual at first glance. However, it essentially serves as a practical experimental setup for investigating a process of scavenging energy from the quantum vacuum, as outlined by the ECE theory [2].

The inventor in [1] claims that the magnetic mill generates useful output power in the kilowatt range. Additionally, it is worth noting that this assembly represents an evolution of earlier work involving transparent, fully open, low-power prototypes [3]<sup>1</sup>.

As a sequel to [4], analysis of [1] is advanced in the present paper, with the aim of evaluating if mechanical vibrations could provide a means of transferring energy to the mill shaft.

We start in Section II by reviewing the setup assemblage. In Section III, we derive expressions for the global forces actuating on the magnets, on the basis of an extended Lorentz Force law that takes elementary magnetic dipole moments into account. Next, owing to the low rigidity of the assembled structure, we show in Section IV that the rotor angular vibrations, which are dynamically generated proportionally to radial force acceleration, could add net mechanical energy to the rotating parts. Finally, we conclude the analysis in Section V, including a numerical example to verify that the calculated rotor angular vibrations have realistic small values, as expected.

### II. A PECULIAR EXPERIMENTAL SETUP

The flux mill in [1] has a hollow cylindrical rotor that is assembled from a thin-metal can, and a hinge-like split stator surrounding the rotor. On the rotor's surface, 64 PM disks (short cylindrical-shaped permanent magnets) are fixed in helix staggering (4 rings with 16 magnets per ring). The 2-part stator has also 64 magnets in total (4 rings per part, 8 magnets per split ring), facing the rotor magnets with the same magnetic polarity.

The two parts of the stator are joined together by a non-rigid clip, which leads to small mechanical vibrations during operation. All magnet disks have the same dimensions (5mm/2mm), with some iron filings around to facilitate crossing when magnets meet during rotation. Moreover, a flywheel is added to the rotor shaft to smooth rotational speed.

As sketched in the Appendix, the flux mill shaft is mechanically driven by a belt coupled to the shaft of a 127VAC single-phase motor (washing-machine motor type). This motor is electrically fed by one of the two AC outlets of a DC/AC power electronic inverter (from 12V DC to 110V/60Hz square-wave AC).

In turn, the electronic inverter's 12VDC inlet is powered by the rectified DC voltage from an alternator (a automobile starter motor/generator), while a 12V battery is also linked in parallel to the same DC contacts. Finally, the alternator's shaft is also belt-coupled to the flux mill shaft.

Altogether, we have a loop concerning energy circulation, where the expected prime-mover is the magnetic flux mill.

To begin with operation, the electronic inverter DC voltage is set by the 12V battery, in order to bring all the shafts up to nominal speed (as in an automobile). Subsequently, the battery cables are disconnected. From this moment on, there are no other conventional sustainable power sources in the setup.

After reaching stable operation, a variety of loads are connected to the electronic inverter's second AC outlet (like light bulbs, drills, electric saw, etc.), and enough energy is unfolded, as shown in the video.

Given the "vibrational" approach stated in [4], there should be an additional, exterior magnetic field in the environment of the flux mill, other than the own magnetic fields created by the stator and rotor magnets.

This external B field is evoked from spacetime resonances, and has a circularly polarized flux density waveform with general expression (in ccw convention):

$$\vec{B}_{ext} = B_S [\cos(\kappa z - \omega t) \vec{a}_x - \sin(\kappa z - \omega t) \vec{a}_y], \quad (1)$$

where  $\vec{a}_x, \vec{a}_y$  are orthonormal vectors referenced to a stationary frame, and  $\omega$  the rotor shaft angular velocity. In the case of a rotor with radius  $r_C$  and height  $h_C$ , where  $n$  equally separated rings with  $\eta$  magnets per ring are inlaid, the wavenumber  $\kappa$  in (1) is found to become

$$\kappa = \frac{n-1}{\eta} \frac{\pi}{h_C}. \quad (2)$$

<sup>1</sup>The results obtained in this paper are also relevant for [3].



Without loss of generality,  $z_C \equiv 0$  is chosen for (8), meaning that the focus is just in one of the stator magnet rings.

#### A. Magnetic force components

Defining

$$\mathcal{F} = \vec{\mu}_C \cdot \vec{B}_{\text{ext}}, \quad (10)$$

it follows from (6) and (8) that

$$\mathcal{F} = \mu_C (B_S + B'_S \cos(\eta\phi)). \quad (11)$$

Correspondingly, the resulting force on the magnetic dipole moment  $\vec{\mu}_C$  is obtained with reference to (7) :

$$\vec{F}_C = \vec{\nabla} \mathcal{F}. \quad (12)$$

The required gradients in (12) can be calculated as function of the rotation angle  $\phi$  with

$$\vec{F}_C = \frac{\partial \mathcal{F}}{\partial x_S} \vec{a}_x + \frac{\partial \mathcal{F}}{\partial y_S} \vec{a}_y, \quad (13)$$

where, from (11),

$$\frac{\partial \mathcal{F}}{\partial \phi} = -\eta \mu_C B'_S \sin(\eta\phi), \quad (14)$$

and, in regard to (5),

$$\begin{aligned} \partial x_S / \partial \phi &= -r_C \sin \phi, \\ \partial y_S / \partial \phi &= r_C \cos \phi. \end{aligned} \quad (15)$$

Respecting cylindrical coordinates,  $\vec{F}_C$  is given by

$$\begin{aligned} \vec{F}_C &= F_r \vec{a}_r + F_\phi \vec{a}_\phi, \\ F_r &= F_x \cos \phi + F_y \sin \phi, \\ F_\phi &= -F_x \sin \phi + F_y \cos \phi. \end{aligned} \quad (16)$$

After substitution of (15) into (13), it follows from (16) that

$$\begin{aligned} F_r &= \frac{\partial \mathcal{F}}{\partial \phi} \frac{\cos \phi}{-r_C \sin \phi} + \frac{\partial \mathcal{F}}{\partial \phi} \frac{\sin \phi}{r_C \cos \phi} \\ &= -\frac{2}{r_C} \frac{\partial \mathcal{F}}{\partial \phi} \frac{\cos(2\phi)}{\sin(2\phi)}, \end{aligned} \quad (17)$$

$$\begin{aligned} F_\phi &= -\frac{\partial \mathcal{F}}{\partial \phi} \frac{\sin \phi}{-r_C \sin \phi} + \frac{\partial \mathcal{F}}{\partial \phi} \frac{\cos \phi}{r_C \cos \phi} \\ &= \frac{2}{r_C} \frac{\partial \mathcal{F}}{\partial \phi}, \end{aligned} \quad (18)$$

which leads to, in view of (14),

$$F_r = F_0 \frac{\sin(\eta\phi) \cos(2\phi)}{\sin(2\phi)}, \quad (19)$$

$$F_\phi = -F_0 \sin(\eta\phi), \quad (20)$$

with

$$F_0 = 2 \frac{\eta \mu_C B'_S}{r_C}. \quad (21)$$

A plot of (19)-(20) for  $\eta = 16$  is shown in Fig. 2. It can be seen that the magnet assembly geometry brings about impulsive acceleration for the radial forces<sup>4</sup>.

<sup>4</sup>Asymptotic behaviour of (19).

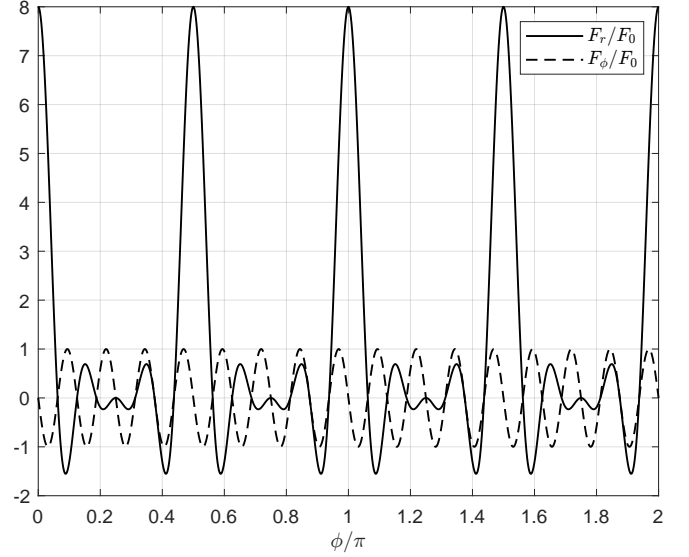


Fig. 2: Radial ( $F_r$ ) and rotational ( $F_\phi$ ) forces. Normalized Eqs.(19)-(20) with  $\eta = 16$ .

#### B. Rotor angular vibration

The vibrating rotational angle,  $\phi'_S$  in Fig. 1, is due to the superposition of a variety of mechanical perturbations. Be that as it may, a primary assumption in this paper is to consider that  $\phi'_S$  has a component that is *dynamically* aroused by the acceleration of *radial forces* in the flux mill.

Therefore, since stator and rotor radial forces are similar, an expression for infinitesimal increments of  $\phi'_S$  is written as

$$d\phi'_S = \lambda \frac{\partial F_r}{\partial \phi} d\phi, \quad (22)$$

where  $\lambda$  is a constant of proportionality, intrinsic to the assemblage mechanical rigidity, and, with reference to (19),

$$\frac{\partial F_r}{\partial \phi} = -F_0 \left[ 2 \frac{\sin(\eta\phi)}{\sin^2(2\phi)} - \eta \frac{\cos(\eta\phi) \cos(2\phi)}{\sin(2\phi)} \right]. \quad (23)$$

A plot of (23) for  $\eta = 16$  is illustrated in Fig. 3.

Owing to (22), the vibrating rotational angle is determined with

$$\phi'_S = \lambda \int \frac{\partial F_r}{\partial \phi} d\phi, \quad (24)$$

and its peak-to-peak magnitude,  $\Delta\phi'_S$ , ascertained from

$$\Delta\phi'_S = \max(\phi'_S) - \min(\phi'_S), \quad 0 \leq \phi \leq 2\pi. \quad (25)$$

#### C. Energy increments

Work is done by  $F_\phi$ , the angular force component in (20), upon the dipole moment  $\vec{\mu}_C$  at each linear increment  $d\phi'_S$ . Since  $\vec{\mu}_C$  is located with radius  $r_C$  around a pivot axis, a infinitesimal energy increment equal to

$$dQ'_S = F_\phi r_C d\phi'_S \quad (26)$$

is, therefore, added to the rotating system parts.

In relation to (18) and (22), (26) is found to become

$$dQ'_S = 2\lambda \left( \frac{\partial \mathcal{F}}{\partial \phi} \right) \left( \frac{\partial F_r}{\partial \phi} \right) d\phi. \quad (27)$$

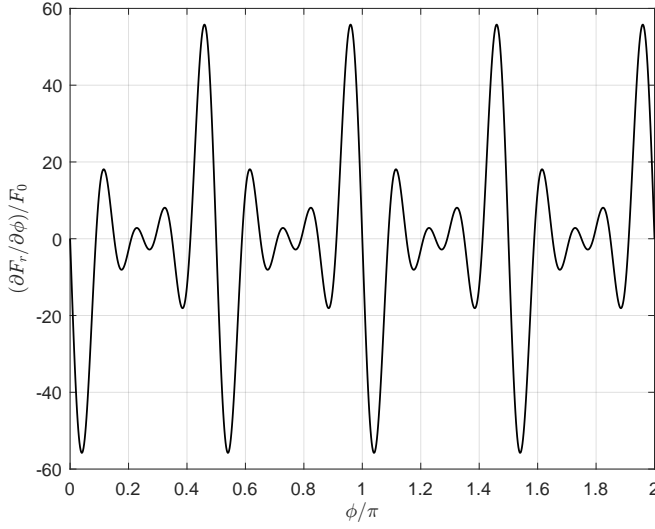


Fig. 3: Rate-of-change of the radial force in Fig.(2). Normalized Eq.(23) with  $\eta = 16$ .

Taking (14) and (23) into account, after some manipulations it results from (27) that

$$\frac{\partial Q'_S}{\partial \phi} = Q_0 \frac{\sin(\eta\phi)}{\sin(2\phi)} \left[ 2 \frac{\sin(\eta\phi)}{\sin(2\phi)} - \eta \cos(\eta\phi) \cos(2\phi) \right] \quad (28)$$

with

$$Q_0 = 8 \frac{\lambda(\eta\mu_C B'_S)^2}{r_C}. \quad (29)$$

A plot of (28) for  $\eta = 16$  is shown in Fig. 4. It can be seen that the average of  $\partial Q'_S/\partial \phi$  is not zero. Asymmetry in the energy transfer to the rotating shaft occurs mainly about the regions with impulsive acceleration (see Fig. 2). As a consequence,

$$Q'_S = \int_0^{2\pi} \frac{\partial Q'_S}{\partial \phi} d\phi > 0, \quad (30)$$

meaning that, after each complete turn, a net mechanical energy increase equal to  $Q'_S$  is brought to the rotor shaft.

## V. NUMERICAL EXAMPLE

The primary parameter for quantification of the analysis in the previous sections is  $B'_S$ , the oscillating magnitude of the magnetic flux aroused by mechanical vibrations.

If a working setup is available for open research, it should be possible to measure the value of  $B'_S$ . Alternatively, if  $\Delta\phi'_S$  is measured (the peak-to-peak magnitude of the angular vibration), the value of  $B'_S$  can be fetched by try-and-error iterations, following the procedure below. Based on the value of  $B'_S$ , all the other coefficients for the previous equations can be obtained.

The geometric dimensions from Table 1 are applied in the sequence, being similar to the ones in [1].

For instance, if it is desired to have a flux mill that delivers  $P=500\text{W}$  mechanical power out of the rotor shaft at 1000rpm, the necessary total mechanical energy per turn, say  $Q_\Sigma$ , at  $\omega = \frac{2\pi}{60}1000$  [rad/s], should be

$$Q_\Sigma = P/\omega = 4.77 \text{ [J]}. \quad (31)$$

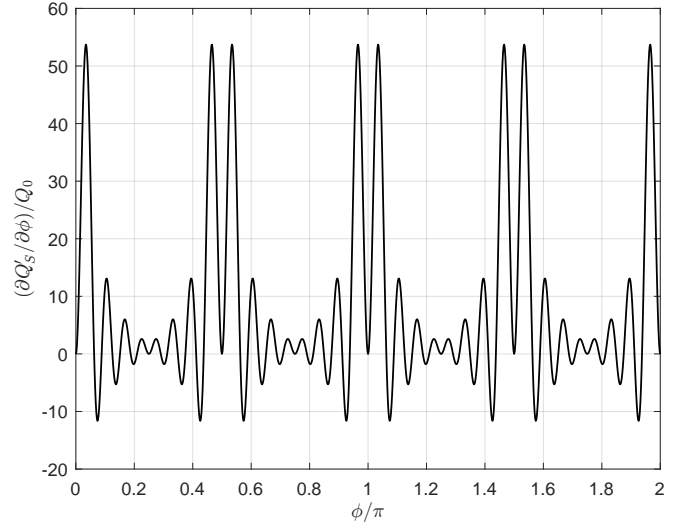


Fig. 4: Oscillations in energy transfer as function of the shaft angular position. Normalized Eq.(28) with  $\eta = 16$ .

TABLE I: Parameters and geometrical dimensions

Parameter	Value	Description
$B_{re}$	[T]	1.42 remanent magnetization NFeB 52
$R_D$	[mm]	2.5 PM disk radius
$h_D$	[mm]	2.0 PM disk height
$r_C$	[mm]	40 rotor radius
$h_C$	[mm]	45 rotor height
$n$	[-]	4 number of rotor rings with PM's
$\eta$	[-]	16 number of PM's per ring
$P$	[W]	500 rotor mechanical output power
rpm	[turns/min]	1000 shaft rotation speed

Since there are 64 ( $= n \cdot \eta$ ) magnets inlaid on the rotor, the required energy increment per turn per magnet will be

$$Q'_S = \frac{Q_\Sigma}{64} = 74.6 \text{ [mJ]}. \quad (32)$$

Regarding (28), it results for  $\eta = 16$  that

$$\frac{Q'_S}{Q_0} = \frac{1}{Q_0} \int_0^{2\pi} \frac{\partial Q'_S}{\partial \phi} d\phi = 50.27, \quad (33)$$

$$\Rightarrow Q_0 = \frac{1}{50.27} Q'_S = 0.0015. \quad (34)$$

To proceed, an attempt value for  $B'_S$  is needed. Let's try  $B'_S = 80\text{mT}$ , which is a small quantity if, for instance, the remanent flux density of the magnets in Table 1 is taken as reference ( $B_{re} = 1.42\text{T}$ ).

Continuing,

$$F_0 = 2 \frac{\eta\mu_C B'_S}{r_C} = 2.90, \quad (35)$$

$$\lambda = \frac{1}{8 (\eta\mu_C B'_S)^2} Q_0 = 0.0022, \quad (36)$$

and the vibrating angle  $\phi'_S$  is calculated from (24):

$$\phi'_S = \lambda F_r(\phi), \quad 0 \leq \phi \leq 2\pi, \quad (37)$$

as shown in Fig. 5.

At last, inspecting Fig. 5, we get with (25) that

$$\Delta\phi'_S = 0.0195\pi = 3.5^\circ, \quad (38)$$

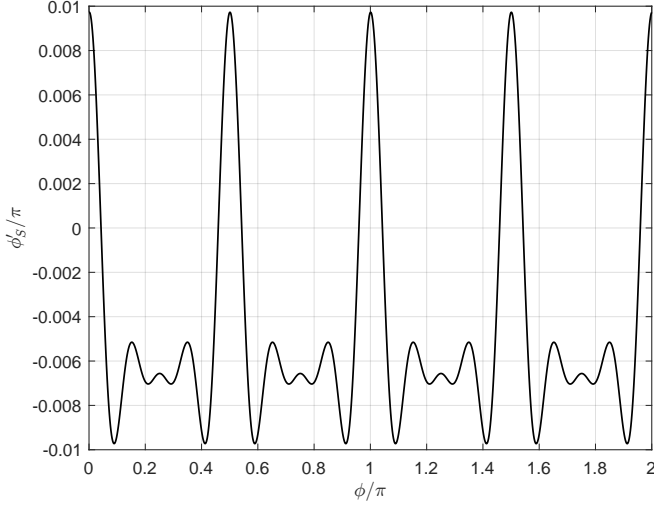


Fig. 5: Angular rotor disturbances. Eq.(24) with  $\eta = 16$  and  $B'_S = 80\text{mT}$ .

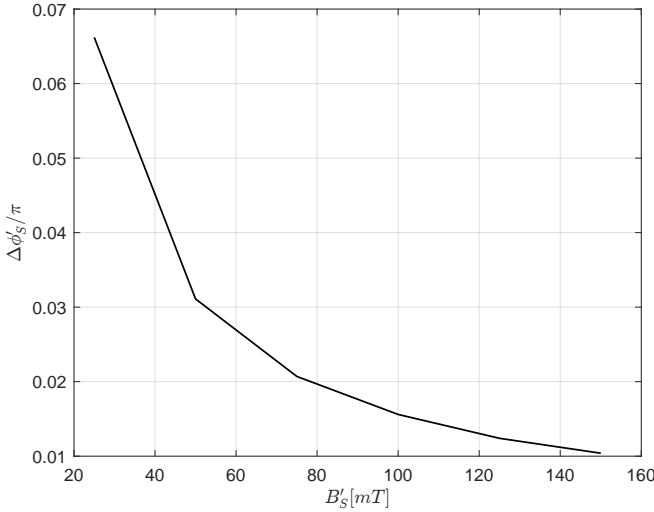


Fig. 6: Peak-to-peak angular vibration magnitude superposed on the rotor shaft, as function of oscillations in the magnetic flux magnitude. Eq.(25) with  $\eta=16$  and  $P=500\text{W}$  at 1000rpm.

confirming that transfer of energy from the quantum vacuum could be realized based on narrow rotational vibrations in the construction of the flux mill.

Fig. 6 shows the sensitivity of  $\Delta\phi'_S$  with respect of  $B'_S$ . The higher  $B'_S$ , the narrower the vibrations needed for generating the same power of 500W at 1000rpm.

## VI. CONCLUSION

Applying the concepts of [4] to the situation of [1], it is hypothesized that mechanical vibrations and magnetic flux oscillations are cooperative in a magnetic-wind mill. The underlying premises are: (a) the magnitude of the external magnetic flux bears an oscillating *radial* component due to the low rigidity of the mechanical construction, and (b) the

rotational motion has a vibrating *angular* component proportional to the *acceleration* of dynamic *radial* forces. In this way, a path is suggested for describing the transfer of energy from the quantum vacuum to the mill shaft.

A numerical example is detailed to check that the calculated peak-to-peak magnitude of the rotor's angular vibration has a small realistic value.

## APPENDIX

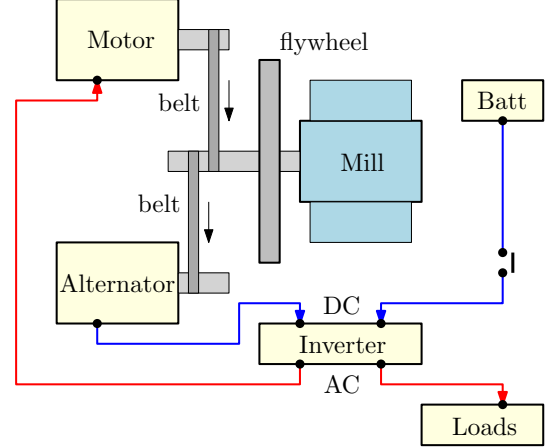


Fig. 7: General arrangement of the setup parts in [1].

## ACKNOWLEDGEMENTS

The personal communications with Horst Eckardt were greatly appreciated.

## REFERENCES

- [1] Dicas do Leao, *Self-sustained energy generator 4kW*, <https://www.youtube.com/watch?v=IBV8Pg0RcII>
- [2] H. Eckardt, *Einstein-Cartan-Evans Unified Field Theory*, Feb 2022, ISBN-13: 978-3754949474
- [3] Dicas do Leao, (a) <https://www.youtube.com/watch?v=pMD-GSjqmc> (b) <https://www.youtube.com/watch?v=HG32MoYXD bw>
- [4] J.L. Duarte, *Essay on magnetic-wind mills, Part II : Staying power from spacetime*, Feb 2023, [https://aias.us/documents/otherPapers/..](https://aias.us/documents/otherPapers/)
- [5] J.A. Barandes, *Can magnetic forces do work?*, Jul 2023, <https://arxiv.org/abs/1911.08890>

First appeared: November 9th, 2024<sup>url</sup>

This version: December 10th, 2024<sup>url</sup>

J.L. Duarte  
magnetogenesis@proton.me